Proceedings of the 16th European VLBI Network Symposium
Ros, E., Benke, P., Dzib, S., Rottmann, I., & Zensus, J.A. (eds.)
September 2nd-6th 2024, Bonn, Germany

Jet properties of FR0 radio galaxies: need for VLBI data

R. D. Baldi[1], G. Giovannini[1,2], A. Capetti[3], and R. Lico[1,4]

[1] INAF - Istituto di Radioastronomia, via Gobetti 101, I-40129 Bologna, Italy
[2] Dipartimento di Fisica e Astronomia, Università di Bologna, Via P. Gobetti 93, I-40129 Bologna, Italy
[3] INAF - Osservatorio Astrofisico di Torino, Strada Osservatorio 20, I-10025 Pino Torinese, Italy
[4] Instituto de Astrofísica de Andalucía-CSIC, Glorieta de la Astronomía s/n, E-18008 Granada, Spain

Abstract. Fanaroff-Riley (FR) type 0 radio galaxies are a subclass of radio-loud active galactic nuclei (AGN) that lack extended kpc-scale jets, different from the classical FRI and FRII radio galaxies. They constitute the most abundant population of radio galaxies in the local Universe (z<0.1), yet remain largely unexplored. VLBI observations of a limited number of FR0s demonstrated that their central supermassive black hole (SMBH) are able to lunch mostly two-sided jets, with mildly relativistic bulk speed. In this work, we highlight the need of further high-resolution radio observations to probe the jet structures of these compact radio galaxies, by showing exploratory results of our EVN+eMERLIN observation campaign of FR0s. A preliminary analysis of these recent data reveals a possible change of the jet direction at different scales. We shortly discuss their physical conditions to explain the observed jet compactness, stressing the role of the SMBH spin vector in shaping their radio morphology.

1. Introduction

Radio galaxies (RGs) are radio-loud active galactic nuclei (AGN) with misaligned relativistic jets that produce non-thermal emission observable across the electromagnetic spectrum. Typically associated with massive, gas-poor elliptical galaxies, RGs are classified into two categories: Fanaroff-Riley type I (FRI) and type II (FRII), based on radio morphology (Fanaroff & Riley 1974) and Low-Excitation or High-Excitation RGs based on accretion properties (low Eddington ratios <0.01 for LERGs, Best & Heckman 2012; Heckman & Best 2014). FRI sources exhibit edge-darkened jets and are generally LERGs, while FRII sources show edge-brightened jets and can be LERGs or HERGs (Baldi & Capetti 2010; Miraghaei & Best 2017; Grandi et al. 2021; Mingo et al. 2022). Recently, large-scale surveys such as the 1.4-GHz FIRST (Becker et al. 1995), 150-MHz LOFAR (Shimwell et al. 2022), and SDSS optical surveys (Abazajian et al. 2009) have revealed an enormous population of low-luminosity compact RGs ($<10^{24}$ W Hz^{-1}), termed FR0 galaxies, which lacks extended jet emission (Baldi & Capetti 2009; Ghisellini 2011) and does not fit into the traditional FR I/II classification.

In this context, Best & Heckman (2012) selected thousands of low-power RGs ($<10^{22}$ W Hz^{-1}) by cross-matching optical surveys, to search for early-type galaxies, and radio surveys (FIRST), to find radio-band counterpart with flux densities > 5 mJy, more than a factor of 1000 lower than the flux densities of classical FRI/FRIIs commonly considered for RG population studies (e.g., the Third Cambridge Catalog 3C Bennett 1962; Spinrad et al. 1985, >9 Jy at 178 MHz). One key tool to study the nature of this unexplored population is the accretion-ejection diagram (Fig. 1), where proxies for kinetic jet power (L_{jet} from total radio power) and accretion disc power (L_{disc} from the [O III] line luminosity) are used as axes (e.g. Heckman & Best 2014 for a discussion). LERG and HERG populations mark two separate empirical correlations in this diagram, corresponding to two distinct disc-jet couplings, expressed by different ratios, $L_{jet}/L_{disc} \sim$ -1.25 − -0.5. The low-power RG population selected by Best & Heckman (2012) do not fully follow the LERG population unexpectedly, but show a larger scatter of jet power. More precisely, the low-power LERGs with extended jetted morphologies (∼20%) in the FIRST maps follow the LERG correlation, while the majority show a deficit of total radio luminosities by a factor 100 − 1000 with respect to the FRIs at the same accretion luminosity ($\sim10^{40}$ erg s^{-1}). Such a population appears all unresolved (compact) at the scale of 5 arcsec in the FIRST radio maps, which have been named as FR0s (Baldi & Capetti 2010). Their high core dominance is attributed to the lack of extended radio emission rather than an enhanced core, as they have similar core-to-emission line luminosity and the similar nuclear properties compared to FRIs (Torresi et al. 2018; Baldi et al. 2019; Baldi 2023).

Compact radio structure is characteristic of several astrophysical sources. A bona-fide FR0 sample requires strict criteria: i) unresolved on kpc-scale, ii) red early-type galaxies, iii) large SMBH masses ($>10^{7.5}$ $M_\odot$), iv) LERG classification, minimizing spurious sources like star-forming and radio-quiet AGN. Accordingly, Baldi et al. (2018) selected 104 FR0s at $z < 0.05$ with host-SMBH properties similar to LERGs (Heckman & Best 2014). A statistical study of the FR0 hosts properties indicates that jet confinement or mechanical external frustration by the interstellar medium is an unlikely scenario (Baldi 2023).

Compact, small radio structures are generally characteristic of young RGs, marking an early stage in their evolution (Snellen et al. 2000; O'Dea & Saikia 2021). A no-

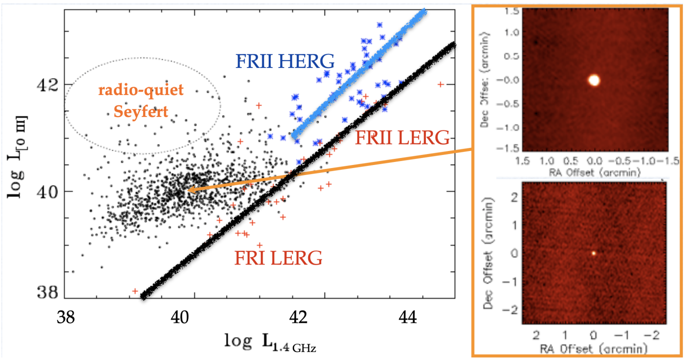

Fig. 1. Accretion-ejection diagram. Total radio luminosity (from 1.4. GHz NVSS maps, Condon et al. 1998) vs. optical [O III] line luminosity (from SDSS, both in erg s^{-1}), used as proxies for the jet and accretion power for the RGs at $z < 0.1$. The two dashed lines reproduce the line-radio correlation followed by LERGs (black line) and HERGs (blue line of the 3CR sample (red pluses and blue asterisks respectively). The ellipse marks the boundaries of the location of radio-quiet Seyfert galaxies (e.g. Whittle 1985). The right panels are two examples of the typical compact radio structures observed with FIRST maps, representative for the bulk of the population of low-power RGs that constitute the FR0 population (Baldi 2023).

table feature of young RGs (ages $<10^6$ yr) is their peaked radio spectra, caused by synchrotron self-absorption at low frequencies, without a flat spectrum at higher frequencies. This produces a peak at a specific turnover frequency, which decreases as the source matures (O'Dea & Baum 1997). Conversely, FR0s show broader and less pronounced spectral curvatures from hundreds of MHz to GHz (Sadler et al. 2014; Capetti et al. 2020) compared to genuinely young RGs like GHz-Peaked RGs. FR0s mostly exhibit flat or slightly convex spectra, with some showing inverted spectra at higher frequencies (Capetti et al. 2019). The high number density of FR0s (five times that of FR Is, Baldi 2023) also challenges the interpretation of the entire FR0 class as young RGs, suggesting instead that additional considerations are needed to place them within the duty cycle and evolutionary scheme of the whole RG population. A large number of FR0s is also expected at high redshifts, given the significant identification of compact RGs observed in deep radio surveys (e.g., Bondi et al. 2018; Radcliffe et al. 2021; Vardoulaki et al. 2021).

1.1. Need for high-resolution radio observations

Multi-band Very Large Array (VLA) observations confirm that the majority of FR0 galaxies exhibit compact radio emission down to $\sim$0.3″, with only about 6 of the 25 sources resolved with kpc-scale jets (Baldi et al. 2015, 2019). The enhanced Multi Element Remotely Linked Interferometer Network (eMERLIN) provides higher resolution down to 0.05″ Combining visibilities of VLA and eMERLIN (probing long and short baselines) reveals the presence of low-brightness sub-kpc jets in two cases, supporting the idea that extended galactic-scale jets may be present in the whole FR0 population but are difficult to detect due to their faintness (Baldi et al. 2021).

The VLBI (Very Long Baseline Interferometry) technique allows to access to pc-scale radio emission, offering crucial insights into FR0 jet properties near the jet-launching site. In fact, long-baseline FR0 observations turned out to be successful to detect low-brightness jet emission. Studies by Cheng & An (2018) and Cheng et al. (2021) using Very Long Baseline Array (VLBA) and the European VLBI Network (EVN) resolved jets in 80% of FR0s, indicating mildly relativistic jet speeds (<0.5c). However, these studies focused on particularly bright FR0s. Giovannini et al. (2023) have targeted less luminous FR0s: VLBA and EVN observations of 18 FR0CAT objects resoved pc-scale jets in most sources (Fig. 1.1).

High-resolution eMERLIN observations detected sub-mJy core components, with pc-scale emission contributing to 3–6% of total kpc-scale emission. Thirty targets have been observed so far with the VLBI technique (VLBA, EVN and eMERLIN). The majority are two-sided (15/30) sources and then one-sided (9/30) and a minority are unresolved (6/30) down to eMERLIN resolution of $\sim$50 mas. Furthermore, jet sidedness analysis suggests that the radio structures in FR0 galaxies are symmetric, confirming the mildly relativistic jet bulk speeds at pc scales, slower than classical FRIs (Giovannini et al. 2023).

The current VLBI observations of FR0s demonstrated the power of this technique in resolving the jet structures of FR0s and highlighted the tremendous need for further high-resolution observations to undertake a statistical study of the whole population.

2. Data

We have recently obtained EVN observations (June 2022, including eMERLIN antenna, EG111 project) for a sample of 6 FR0s in C band in phase-reference mode. The EVN observations were performed with the following array (18 maximum and 9 minimum antennae available per session): Effelsberg, Jodrell Bank, Westerbork, Medicina, Noto, Torun, Onsala, Hartebeesthoek, Irbene, Westerbork, Tianma65, Urumqi, Yebes, Pickmere, Knockin, Defford,

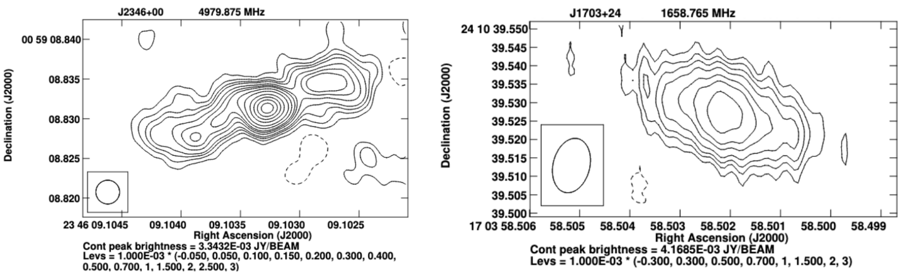

Fig. 2. Examples of VLBI images of two FR0s in L and C band taken from Giovannini et al. (2023).

Darnhall, Cambridge, with a maximum baseline of ∼130 kλ. A bandwidth of 64 MHz was used, divided into 8 intermediate frequency bands, all centred at 4.9 GHz. We obtained observation session of a total time of 4hr/source with at least 2hr on source. The data were processed at the EVN correlator at the Joint Institute for VLBI in Europe (JIVE), in Dwingeloo, The Netherlands. A first post-processing analysis was also carried out at JIVE. A first a priori visibility amplitude calibration was performed using antenna gains and system temperatures measured at each antenna. A fringe fitting of the residual delays and fringe rates was performed for all the radio source using Effelsberg as reference antenna. The phase and amplitude calibration was performed with `AIPS`. We then averaged the data in frequency and exported them to be imaged and self-calibrated in amplitude and phase in `DIFMAP` with cell size of ∼0.3 mas for five sources. The final beam size has a large major axis of ∼1.3 mas (1 mas → 1 pc at z=0.05).

3. Preliminary results

Figure 3 depicts the preliminary maps of five out of the six observed targets (J1025+10, J1040+09, J1213+50, J1230+47, J1559+25). All the sources have been detected with signal-to-noise of higher than 5. The rms generally ranges between 30 and 80 μJy beam^{-1}.

The morphologies are all two-sided structures, apart from J1559+25 which appears compact in full resolution (but resolved with VLBA by Cheng & An 2018). The core flux densities range between 3 and 30 mJy beam^{-1}. The jetted emission appears extended on some tens of mas, which corresponds to some tens of parsec (Fig. 3).

A quick comparison between the radio maps obtained with different arrays (VLA, EVN, eMERLIN) reveals that in two targets the position angle of the extended emission, tracing the jet orientation, changes across the various maps. Figure 3 show the case of J1213+50 whose radio emission elongation in the VLA map (Baldi et al. 2019) on kpc scale is significantly different from that observed at the EVN scale (1.6 GHz, Giovannini et al. 2023) and new EVN+eMERLIN map observed on parsec scale. A more statistically robust analysis of this phenomenon will be performed in a forthcoming paper which will include the study of the whole EG111 program.

4. Conclusions

Current VLBI studies on FR0 RGs provide an interesting insight on the jet properties of this abundant population of radio-loud AGN. A new EVN+eMERLIN high-resolution radio campaign confirms that FR0 *can* launch parsec-scale jets. The jet sidedness and symmetry and proper motion studies point to a mildly-relativist jet bulk speed, lower compared to FRIs and FRIIs. FR0 jets appear to be slower, with Lorentz factors 1−2 at parsec scale, suggesting that relativistic beaming effects are negligible in these sources. In addition, the evident re-orientation of the jet axis at different scale in two cases might indicate the possibility of a crucial role for the SMBH spin in keeping the radio source compact, since jets are launched along the direction of the spin vectors (Stanghellini et al. 2024).

In fact, one possible explanation is that FR0 galaxies host SMBH with low prograde spin, which limits the energy available to launch powerful, extended jets based on a Blandford-Znajek stratified jet model. Over time, as accreting material increases the SMBH's angular momentum, some FR0s might evolve into FRI galaxies by increasing SMBH spin (Garofalo & Singh 2019). Another possibility is that weak magnetic fields at the base of the jet could prevent the formation of large-scale structures, confining the jets to smaller sizes (Grandi et al. 2021). Numerical simulations of a FR0 with a conical jet relativistic profile shows the development of a re-collimation shock which promotes the growth of instabilities and a rapid jet deceleration, resulting in a compact low-power jet morphology (Costa et al. 2024).

Further VLBI studies are needed to investigate on the jet launching/propagation mechanism in this class of intrinsically compact RGs. High-frequency (22-43 GHz) global VLBI observations would be ideal to resolve the inner jet structure. In this framework, the upgrade of the Italian VLBI antennae to the high-frequency band is, indeed, crucial for future studies. Furthermore, X-ray and optical-band studies, along with ad-hoc numerical simulations, will help to better quantify the impact of the FR0 jets on the hosts, and their relationship with the central SMBH properties and unearth the high-z population of FR0s at high redshifts.

Acknowledgements. The European VLBI Network (www.evlbi.org) is a joint facility of independent European, African, Asian, and North American radio astronomy institutes. Scientific results from data pre-

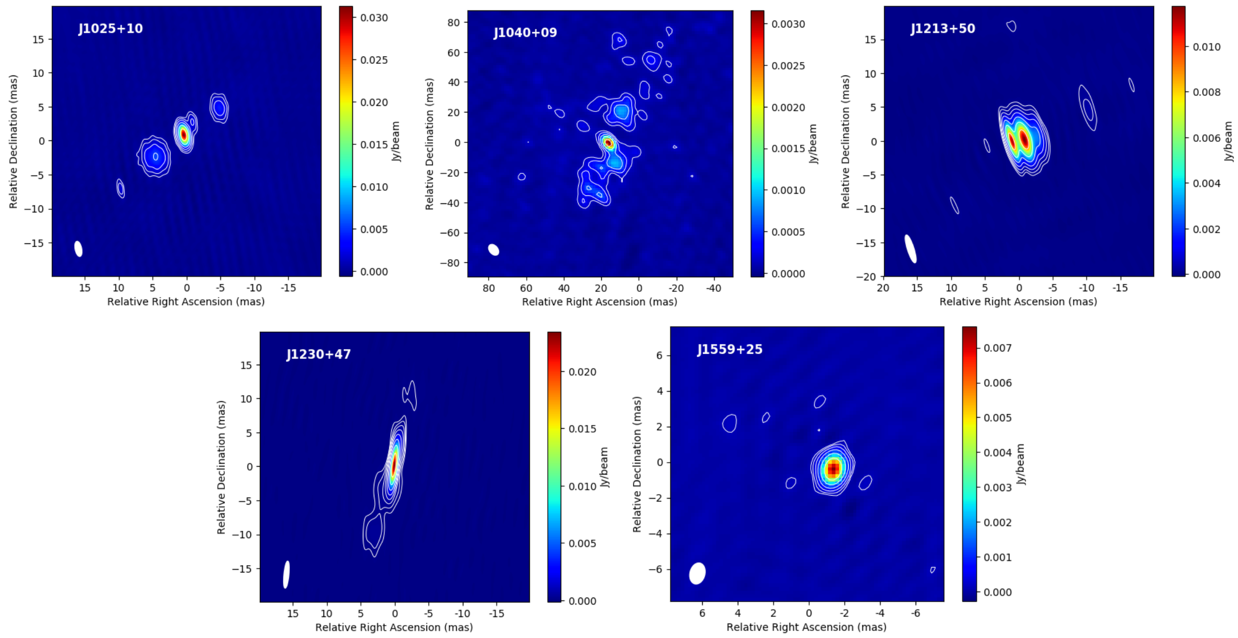

Fig. 3. Preliminary calibrated maps of five (out of six) FR0s observed with EVN+eMERLIN array in C band (EG111 project). The contour levels are measured from the rms ×(1, 2, 4, 8, 16, 32, 64, 128), where the rms ranges between 30 and 80 μJy. The beam is displayed as white ellipse in the left bottom corner.

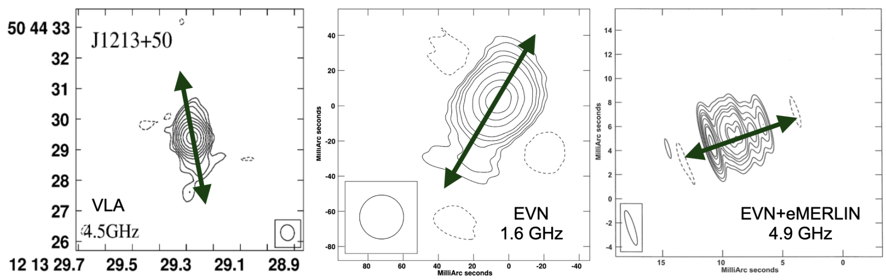

Fig. 4. Panel of three sets of radio maps of the FR0 J1213+50 observed with VLA (4.5 GH, Baldi et al. 2019), EVN (1.6 GHz, Giovannini et al. 2023) and EVN+eMERLIN (new data, 4.9 GHz). The arrow roughly indicates the position angle of the jet direction, which changes a different physical scales across the maps.

sented in this publication are derived from the following EVN project code(s): EG111.

References

Abazajian, K. N., Adelman-McCarthy, J. K., Agüeros, M. A., et al. 2009, ApJS, 182, 543
Baldi, R. D. 2023, A&A Rev., 31, 3
Baldi, R. D. & Capetti, A. 2009, A&A, 508, 603
Baldi, R. D. & Capetti, A. 2010, A&A, 519, A48
Baldi, R. D., Capetti, A., & Giovannini, G. 2015, A&A, 576, A38
Baldi, R. D., Capetti, A., & Giovannini, G. 2019, MNRAS, 482, 2294
Baldi, R. D., Capetti, A., & Massaro, F. 2018, A&A, 609, A1
Baldi, R. D., Giovannini, G., & Capetti, A. 2021, Galaxies, 9, 106
Becker, R. H., White, R. L., & Helfand, D. J. 1995, ApJ, 450, 559
Bennett, A. S. 1962, MmRAS, 68, 163
Best, P. N. & Heckman, T. M. 2012, MNRAS, 421, 1569
Bondi, M., Zamorani, G., Ciliegi, P., et al. 2018, A&A, 618, L8
Capetti, A., Baldi, R. D., Brienza, M., Morganti, R., & Giovannini, G. 2019, A&A, 631, A176
Capetti, A., Brienza, M., Baldi, R. D., et al. 2020, A&A, 642, A107
Cheng, X., An, T., Sohn, B. W., Hong, X., & Wang, A. 2021, MNRAS, 506, 1609
Cheng, X. P. & An, T. 2018, ApJ, 863, 155
Condon, J. J., Cotton, W. D., Greisen, E. W., et al. 1998, AJ, 115, 1693
Costa, A., Bodo, G., Tavecchio, F., et al. 2024, A&A, 682, L19
Fanaroff, B. L. & Riley, J. M. 1974, MNRAS, 167, 31P
Garofalo, D. & Singh, C. B. 2019, ApJ, 871, 259
Ghisellini, G. 2011, in American Institute of Physics Conference Series, Vol. 1381, American Institute of Physics Conference Series, ed. F. A. Aharonian, W. Hofmann, & F. M. Rieger, 180–198
Giovannini, G., Baldi, R. D., Capetti, A., Giroletti, M., & Lico, R. 2023, A&A, 672, A104
Grandi, P., Torresi, E., Macconi, D., Boccardi, B., & Capetti, A. 2021, ApJ, 911, 17
Heckman, T. M. & Best, P. N. 2014, ARA&A, 52, 589
Mingo, B., Croston, J. H., Best, P. N., et al. 2022, MNRAS, 511, 3250
Miraghaei, H. & Best, P. N. 2017, MNRAS, 466, 4346
O'Dea, C. P. & Baum, S. A. 1997, AJ, 113, 148
O'Dea, C. P. & Saikia, D. J. 2021, A&A Rev., 29, 3
Radcliffe, J. F., Barthel, P. D., Thomson, A. P., et al. 2021, A&A, 649, A27
Sadler, E. M., Ekers, R. D., Mahony, E. K., Mauch, T., & Murphy, T. 2014, MNRAS, 438, 796
Shimwell, T. W., Hardcastle, M. J., Tasse, C., et al. 2022, A&A, 659, A1
Snellen, I. A. G., Schilizzi, R. T., Miley, G. K., et al. 2000, MNRAS, 319, 445
Spinrad, H., Marr, J., Aguilar, L., & Djorgovski, S. 1985, PASP, 97, 932
Stanghellini, C., Orienti, M., Spingola, C., et al. 2024, arXiv e-prints, arXiv:2407.02029
Torresi, E., Grandi, P., Capetti, A., Baldi, R. D., & Giovannini, G. 2018, MNRAS, 476, 5535
Vardoulaki, E., Jiménez Andrade, E. F., Delvecchio, I., et al. 2021, A&A, 648, A102
Whittle, M. 1985, MNRAS, 213, 33